frontiers in Forests and Global Change

TYPE Original Research
PUBLISHED 31 August 2026
DOI 10.3389/ffgc.2026.1922886

OPEN ACCESS

EDITED BY
Andrea Westerband,
University of Louisiana at Lafayette,
United States

REVIEWED BY
Eleinis Ávila-Lovera,
The University of Utah, United States
Walid Elfalleh,
Imam Muhammad ibn Saud Islamic University, Saudi Arabia

*CORRESPONDENCE
Norbert Móricz
✉ moricz.norbert@uni-sopron.hu

RECEIVED 29 June 2026
REVISED 13 August 2026
ACCEPTED 14 August 2026
PUBLISHED 31 August 2026

CITATION
Móricz N, Mészáros I, Kern Z, Illés GZ, Eötvös CB, Berki I and Németh TM (2026) Stable isotope insights into contrasting drought-response strategies of five native broadleaf tree species in East Central Europe.
Front. For. Glob. Change 9:1922886.
doi: 10.3389/ffgc.2026.1922886

Stable isotope insights into contrasting drought-response strategies of five native broadleaf tree species in East Central Europe

Norbert Móricz[1]*, Ilona Mészáros[2], Zoltán Kern[3], Gábor Zoltán Illés[1], Csaba Béla Eötvös[1], Imre Berki[4] and Tamás Márton Németh[1]

[1]Department of Ecology and Forest Management, Forest Research Institute, University of Sopron, Sopron, Hungary, [2]Department of Botany, Faculty of Science and Technology, University of Debrecen, Debrecen, Hungary, [3]HUN-REN Research Centre for Astronomy and Earth Sciences, Institute for Geological and Geochemical Research, Budapest, Hungary, [4]Independent Researcher, Sopron, Hungary

Future forest dynamics under climate change will largely depend on the physiological acclimation capacity of the tree species to the increasing environmental stress. We combined carbon and oxygen stable isotope analyses with growth measurements to estimate the effects of atmospheric CO_2 and drought stress on intrinsic water-use efficiency (iWUE) and secondary growth in five coexisting tree species (*Acer campestre*, *Fraxinus ornus*, *Quercus cerris*, *Quercus pubescens*, *Tilia tomentosa*) in Central Hungary. Generalized additive models explained most of the variation in iWUE (adjusted R^2 = 0.77) and growth (adjusted R^2 = 0.75). The isotope and iWUE chronologies showed that these species experienced increasing hydroclimatic stress, driven primarily by rising temperatures and vapor pressure deficit. The 12-month water balance (WB12), calculated from the previous September to the current August, was the strongest climatic predictor, showing strong correlations with both $\Delta^{13}C$ (r = 0.55–0.73) and iWUE (r = −0.60 to −0.80). Although the species differed in their physiological adaptations, the general pattern of increased iWUE coupled with stagnant or declining growth suggests that elevated atmospheric CO_2 could not fully offset the unfavorable effects of increased warming and drying on tree function. Unlike the other species, *Q. cerris* exhibited only a modest increase in iWUE until around 2010, followed by a more pronounced increase thereafter. The relationships between iWUE and growth reveal fundamental differences among the species in their drought-response strategies. *T. tomentosa* and *F. ornus* appear to adopt a more conservative water-use strategy with strongly increasing iWUE and declining growth which may enhance short-term survival but increase long-term vulnerability. In contrast, *Q. pubescens* and *A. campestre* maintained growth under increasing iWUE, suggesting broader hydraulic safety margins or deeper rooting. *Q. cerris* presented an intermediate pattern with stable growth initially, but pronounced decline under severe drought. Beyond these physiological differences, site conditions and landscape structure also appeared to modulate tree responses through local microclimate effects, including evaporative demand. These findings suggest that the forest composition may shift in the drier regions of Central Europe because coexisting species differ markedly in their capacity to withstand increasing drought stress.

10.3389/ffgc.2026.1922886

KEYWORDS

drought response, intrinsic water-use efficiency, minor native tree species, Quercus, stable isotopes, tree physiology

1 Introduction

Increased warming and drying, together with the continuous rise in atmospheric CO_2 concentration, is already significantly affecting forests in Central Europe: tree radial growth is declining, tree mortality is increasing, and forest decline episodes are becoming more frequent (Móricz et al., 2018; McDowell et al., 2020; Bosela et al., 2021; Knutzen et al., 2025). While radial growth provides valuable information about long-term tree growth and carbon allocation, stable isotopes offer mechanistic insights into plant physiological processes such as photosynthesis and transpiration, as well as the interaction between the tree and the environment. In favorable, non-limiting environments, stable isotopes often provide a more sensitive indicator of climatic variability than radial growth alone (Hartl-Meier et al., 2015).

The intrinsic water-use efficiency (iWUE) is defined as the ratio of CO_2 assimilation rate and the stomatal conductance of water vapor (Osmond et al., 1980; Ehleringer et al., 1993; Saurer and Voelker, 2022). It expresses how much carbon the plant is able to sequester per unit water loss. The stable carbon isotope composition ($\delta^{13}C$) of tree rings is a good proxy to estimate iWUE (Frank et al., 2015; Dorado-Liñán et al., 2020). During favorable, non-limiting conditions, the stomata are more open, hence the intercellular CO_2 concentration in the leaves increases. As a result, the enzyme Rubisco discriminates more strongly against ^{13}C, leading to more negative $\delta^{13}C$ values and lower iWUE. In contrast, during droughts or high vapor pressure deficit (VPD) periods, the stomata close, the intercellular CO_2 concentration decreases, the discrimination against ^{13}C weakens, therefore, $\delta^{13}C$ values become less negative and the iWUE increases (Grossiord et al., 2020). The long-term decline in tree-ring $\delta^{13}C$ values largely reflects the progressive depletion of atmospheric CO_2 in ^{13}C caused by fossil fuel emissions (Leuenberger, 2007). To isolate the physiological signal from this atmospheric trend, carbon isotope discrimination ($\Delta^{13}C$) is calculated by correcting tree-ring $\delta^{13}C$ values for the concurrent atmospheric $\delta^{13}C$ composition (Belmecheri et al., 2022).

In addition to the carbon isotopes, the oxygen isotope ratio, $\delta^{18}O$ provides complementary information about the water status of the plants. While $\delta^{13}C$ values mirrors primarily stomatal behavior and carbon assimilation, $\delta^{18}O$ value is determined mainly by leaf water enrichment that depends on the evaporative demand and source water signals. During periods of high VPD or reduced stomatal conductance, leaf water becomes enriched in heavy isotopes that results in higher $\delta^{18}O$ values. In this way, it helps disentangle whether variation in $\delta^{13}C$ is primarily driven by stomatal closure or by changes in photosynthetic capacity (Scheidegger et al., 2000).

The long-term increase of iWUE has been demonstrated globally at the whole-plant level by numerous studies, based on carbon isotope discrimination (Peñuelas et al., 2008; Li et al., 2017; Mathias and Thomas, 2021). This increase can stem from intensified CO_2 assimilation (Guerrieri et al., 2019; Mathias and Thomas, 2021), decreased stomatal conductance (Saurer et al., 2014; Lévesque et al., 2014) or both. The higher atmospheric CO_2 can stimulate photosynthesis and increase iWUE, which in turn may support tree growth (Giammarchi et al., 2017; Moore et al., 2021). However, drought and high VPD limit tree growth by reducing carbon assimilation due to stomatal closure (Ainsworth and Rogers, 2007; Keenan et al., 2013; Tognetti et al., 2014; Grossiord et al., 2020). Under prolonged or severe drought, the stomatal closure may entirely offset the favorable effect of high CO_2 (van der Woude et al., 2023).

The effect of climate change is largely dependent on the acclimation ability of the species (Enderle et al., 2024). Therefore, it is crucial to better understand the differences in the acclimation capacity of the species to estimate more precisely their vulnerability under increasing atmospheric CO_2 levels and more frequent droughts (Lindner et al., 2010; Sarris et al., 2013). Species differ in their gas-exchange strategies and their capacity to acclimate to elevated CO_2 and recurring drought (Huang et al., 2007; Andreu-Hayles et al., 2011; Linares and Camarero, 2012; Wang and Wang, 2021). Although several studies examined the relationship between iWUE and tree growth for drought-sensitive, temperate species under increasing CO_2 and increasing drought (Linares and Camarero, 2012; Granda et al., 2014; Hereş et al., 2014; Lévesque et al., 2014; Dorado-Liñán et al., 2020), little is known about the physiological responses of many minor deciduous tree species common in Central Europe. Moreover, comparative isotope-based assessments of multiple co-occurring broadleaf species growing under the same climatic conditions remain scarce. Besides species-specific differences, local site conditions and surrounding landscape structure may also influence tree physiological responses by modifying the microclimate, although these effects have received considerably less attention.

In this study, we combined carbon and oxygen stable isotope analysis with radial growth data to evaluate the effects of increasing atmospheric CO_2 and drought stress on iWUE and basal area index (BAI) of five co-existing tree species (*A. campestre L., F. ornus L., Q. cerris L., Q. pubescens Willd., T. tomentosa* Moench) in dry regions of central Hungary. Unlike previous studies focused mainly on dominant tree species, our approach enables direct comparison of physiological acclimation strategies among five co-occurring broadleaf species under comparable climatic conditions. Our previous work in the same area demonstrated that these species exhibited generally high drought resilience, although important interspecific differences were observed (Móricz et al., 2025). Diffuse-porous tree species (*A. campestre, F. ornus, T. tomentosa*) showed high growth sensitivity to climatic variability, while the ring-porous oak species (*Q. cerris, Q. pubescens*) revealed more stable growth, suggesting a lower sensitivity to climatic variability. These differences may relate to differing water-use strategies and may appear in species-specific isotopic signals ($\delta^{13}C$, $\delta^{18}O$) and in iWUE. The combination of radial growth and isotopic data therefore provides a mechanistic framework for understanding how the coexisting species respond to increasing drought and atmospheric CO_2 concentration. Our

10.3389/ffgc.2026.1922886

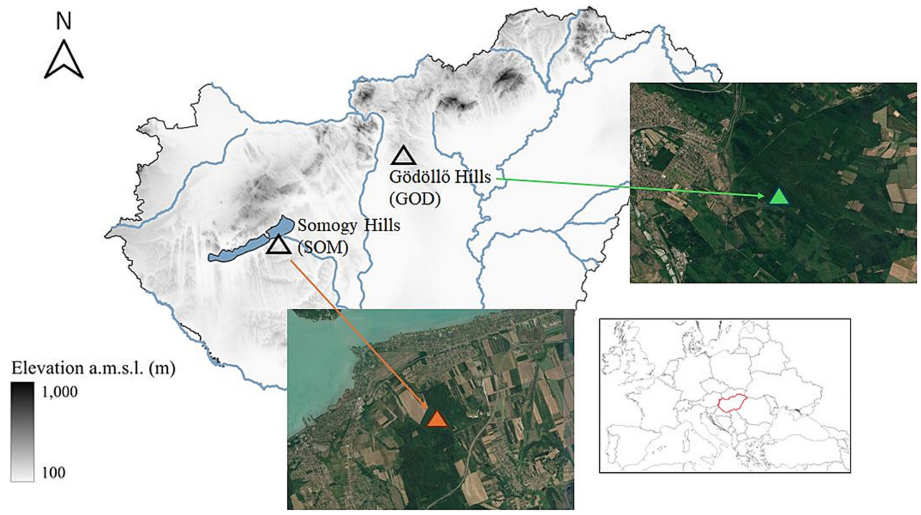

FIGURE 1
Study sites in Hungary (Gödöllő Hills, GOD; Somogy Hills, SOM), the color shaded map shows the elevation above mean sea level (m). The enlarged study sites are displayed at identical scale. Satellite imagery: Google Maps, accessed June 2026, imagery ©2026 Airbus, CNES/Airbus, Landsat/ Copernicus, Maxar Technologies; map data ©2026 Google; adapted by the authors.

specific aims were to (1) compare the temporal changes of BAI, $\Delta^{13}C$, $\delta^{18}O$ and iWUE, (2) explore the relationship among $\Delta^{13}C$, $\delta^{18}O$ and climatic variables, and (3) determine how the BAI and iWUE respond to increasing atmospheric CO_2 and drought stress for the tree species.

2 Materials and methods

2.1 Site description

Two study sites (Gödöllő Hills—GOD; 47.58 N/19.42E and Somogy Hills—SOM; 46.86 N/17.94E) were designated for the analysis in the central part of Hungary (Figure 1).

The climate at both locations is characterized as continental, with annual precipitation between 562 mm (GOD) and 632 mm (SOM) in the period 1971–2022. Mean annual temperature is similar at both sites with 9.5–10.3 °C. None of the sites has access to groundwater, and both are situated at elevations between 215 m (SOM) and 300 m (GOD) above mean sea level (Móricz et al., 2025). The genetic soil type is Cambiosol (brown earth) at both locations (Supplementary material 1).

For this study, we designated one species-rich mixed forest stand at both selected sites (GOD and SOM, Figure 1). The two sites were selected from our previous study network because they represent the driest mixed broadleaf forests investigated, where drought-related growth decline and physiological responses are expected to be most pronounced. The site at GOD is part of a larger forest area in Gödöllő Hills, while the site at SOM is surrounded by agricultural areas from multiple directions at a distance of 500 to 1,000 m. Mean tree age is between 50 and 67 years at the GOD site and between 42 and 47 years at the SOM site. For detailed stand characteristics, see also Móricz et al. (2025). Four tree species (*A. campestre*, *F. ornus*, *Q. pubescens*, *Q. cerris*) were sampled at GOD, while *T. tomentosa* and *Q. cerris* were sampled in SOM, commonly found in Central European broadleaf mixed forests (Caudullo and de Rigo, 2016; de Rigo et al., 2016; Eaton et al., 2016; Pasta et al., 2016; Zecchin et al., 2016). The five species were selected because they are among the dominant broadleaf species of the investigated mixed forests and had previously been analyzed dendrochronologically (Móricz et al., 2025), providing an opportunity to directly compare growth and isotope-based physiological responses within the same study system. To minimize the impact of forest management practices—such as selective thinning and regeneration cutting - on ecophysiological-climate relationships, we selected forest stands with low management intensity over the past few decades. Additionally, to reduce competition, we avoided selecting suppressed trees, as they exhibit larger growth responses to various interventions compared to trees in the upper canopy (Nowacki and Abrams, 1997).

2.2 Climate data

Meteorological data were obtained from the HUCLIM daily gridded climate dataset of the Hungarian Meteorological Service (HMS, 2025)[1]. The daily station data are quality controlled, homogenized by the MASH method (Szentimrey, 2024) and then were interpolated to a regular grid with a spatial resolution of 0.1° using the MISH algorithm (Szentimrey and Bihari, 2014). This dataset has an approximate spatial resolution of ~10 km and covers the period from 1971 to 2022. We assigned the nearest grid points to the study sites and aggregated daily mean temperatures, total precipitation and relative humidity into monthly averages. To account for the elevation differences between the study sites and the corresponding grid points, we adjusted the mean monthly

1 https://odp.met.hu/

temperature data using long-term monthly elevation gradients (Péczely, 1979).

The monthly water balance (WB) was calculated as the difference between precipitation and potential evapotranspiration, following the method described by McCabe and Markstrom (2007). WB effectively reflects the negative impacts of increased temperatures on water availability (Vitasse et al., 2019). We calculated cumulative water-balance indices over different time windows (3–12 months), including a 12-month water balance (WB12) calculated backward from August of the current year of growth. We used WB12 because it showed one of the strongest relationships with tree radial growth in previous studies (e.g., Móricz et al., 2025). VPD was computed using relative humidity and air temperature for the main growing season (June–August). From temperature, we first calculated saturation vapor pressure, and then used it together with relative humidity to derive VPD (Murray, 1967). To characterize potential differences in site-level microclimatic conditions, we used actual evapotranspiration (AET) data at 1-km spatial resolution during the severe drought period 2000–2003 (Szilágyi and Kovács, 2010). AET is a good indicator of available soil moisture and it was calculated for the summer months by averaging the values of pixels of the site locations and their neighbors.

2.3 Sample collection

Five dominant and representative trees were selected for the species present at both sites, and one increment core per tree was collected at breast height (1.3 m) using a 5.15-mm increment borer (Haglöf, Långsele, Sweden). The cores were air-dried, mounted, and sanded to a fine surface. High-resolution digital images were then acquired, and annual ring widths were measured on the images using the WinDENDRO image analysis system (Regent Instruments Inc., Quebec, Canada). Crossdating was first performed visually and subsequently verified using the COFECHA software (Holmes, 1983) to ensure accurate calendar-year assignment of each ring. Basal area increment (BAI) was calculated for each tree and subsequently averaged for each species at both sites using Equation 1:

$$BAI_t = \pi\left(r_t^2 - r_{t-1}^2\right) \quad (1)$$

where r_t and r_{t-1} are the measured stem radii at year t and the preceding year, respectively, and BAI_t is the basal area increment for year t. BAI was calculated in outward direction and the number of missing rings to the pith was approximated using the diameter and core length of each tree with the radius-length method (Norton et al., 1987).

Following ring-width measurements, individual annual rings were excised from each core for stable isotope analyses. In the ring-porous species, annual rings were separated into earlywood and latewood based on their anatomical characteristics under a microscope. Because latewood is formed predominantly from current-year photoassimilates, whereas earlywood contains a greater proportion of remobilized carbon from previous growing seasons (Kagawa et al., 2006; Kimak and Leuenberger, 2015), only the latewood fraction was retained for isotope analysis. The only exception was *A. campestre*, for which earlywood and latewood could not be reliably separated; therefore, the entire annual ring was used. Finally, the ring material representing the same calendar year from the five sampled trees of each species was pooled into a single Eppendorf tube and stored until laboratory analyses. Consequently, one composite isotope sample was analyzed per species and year, rather than individual tree replicates. The five dominant trees were selected to represent the common stand-level isotope signal while keeping the analytical workload feasible over the approximately 50-year chronology. Pooling material from 4 to 5 trees is an established and widely applied approach in tree-ring isotope studies (Leavitt, 2010; Loader et al., 2013).

2.4 Cellulose extraction, stable carbon isotope and intrinsic water-use efficiency determination

Cellulose extraction was applied to remove any effects from changing wood composition (Helle et al., 2022). Alpha-cellulose was separated by the modified Jayme-Wise method (Loader et al., 1997) and homogenized by a standard ultrasonic protocol (Laumer et al., 2009). For the simultaneous measurements of carbon and oxygen isotope ratios, ~0.2 mg of α-cellulose was packed in Ag-foil capsules and pyrolyzed over glassy carbon at 1450 °C (Leuenberger and Filot, 2007) using a ThermoQuest TC-EA interfaced with a Thermo Delta V Advantage IRMS (Kern et al., 2022). All results were expressed as ‰ relative to a standard (VPDB for $\delta^{13}C$ and VSMOW for $\delta^{18}O$). Each sample was measured in triplicate, and internal standards were measured as unknown after measurements of every five real samples. The mean bias (0.02‰ for $\delta^{13}C$; 0.01‰ for $\delta^{18}O$) and analytical precision (0.07‰ for $\delta^{13}C$ and 0.09‰ for $\delta^{18}O$) calculated from repeated ($n = 125$) measurements of the QA standard (Supplementary material 1) is well within the long-term analytical reproducibility of the laboratory (Kern et al., 2022). A decline in the raw $\delta^{13}C$ chronologies is attributed to the progressive decrease of atmospheric $\delta^{13}C$ due to the combustion of fossil fuels (Leuenberger, 2007). This trend was removed in the carbon isotope chronology using the annual records of past atmospheric $\delta^{13}C$ (Belmecheri et al., 2022) to obtain carbon discrimination ($\Delta^{13}C$).

The iWUE is related to the loss of water from plants via their stomata and is a function of the amount of water lost per unit of CO_2 assimilated. iWUE was calculated using the simplified linear model of Farquhar et al. (1982) as the ratio of the net carbon gain (A) versus leaf conductance for water vapor (g_s), as follows (Equation 2):

$$iWUE = \frac{A}{g_s} = C_a \times \frac{b - \Delta^{13}C}{1.6 \times (b - a)} \quad (2)$$

where C_a is the atmospheric CO_2 concentrations, a (=4.4‰) refers to the slower diffusivity of $^{13}CO_2$ relative to $^{12}CO_2$ in air, b (=27‰) is the isotopic fractionation caused by enzymatic C fixation, and *1.6* is the ratio between the diffusivities of water vapor and CO_2 in the air. $\Delta^{13}C$ and iWUE were calculated using the isocalcR package (Mathias and Hudiburg, 2022).

2.5 Statistical analysis

Pairwise differences in long-term mean values (50-year period) of BAI, $\Delta^{13}C$, $\delta^{18}O$ and iWUE among species and sites were assessed using independent-samples t-tests. The temporal trends of these variables complemented with climatic variables were examined using the

10.3389/ffgc.2026.1922886

non-parametric Mann-Kendall test for the period 1971–2022. As time series often include autocorrelation, we used the trend-free pre-whitening (TFPW) version of the test, which considers the autocorrelation before estimating the Mann-Kendall statistics (Yue et al., 2002). This approach provides a more reliable evaluation of the monotonic trends, since it reduces the significance level evoked by the temporal autocorrelation. To quantify the magnitude of the monotonic trends, we also calculated Sen's slope, which provides a robust, non-parametric estimate of the trend slope (Sen, 1968).

We compared the species-specific $\delta^{18}O$ anomalies calculated for drought years and for wet years. WB12 was used to select the drought years and wet years. Years falling below the 25th percentile were classified as drought years (10 years), whereas those above the 75th percentile were considered wet (12 years). The raw $\delta^{18}O$ time series were detrended to remove the long-term, non-climatic trends and the residuals were used for comparison and visualization.

The relationships of $\Delta^{13}C$, $\delta^{18}O$ and iWUE with climatic variables (monthly precipitation, temperature and water balance) were assessed by Pearson correlation for each species. We analyzed the effect of climatic variables from June of the previous year until September of the current year of ring formation using the treeclim package (Zang and Biondi, 2015) in R software (R Core Team, 2026). Additionally, correlations with WB were computed for 3- to 12-month windows starting from August of the current year and extending backward to September of the previous year. For VPD, we calculated the correlation coefficient for the summer months of each year. Additionally, we computed the correlations between $\Delta^{13}C$ and $\delta^{18}O$ data for all species and sites to further elaborate the physiological background of the species. Because the monthly climate variables are temporally correlated and the analyses were intended to identify climatic response patterns rather than test a set of independent hypotheses, no formal multiple-testing correction was applied. We tested the significance of correlations using bootstrap resampling (Zang and Biondi, 2015).

We applied generalized additive models (GAM) to explore the environmental and physiological drivers of (i) iWUE and (ii) to examine how the variation in iWUE affects tree growth, expressed by BAI. We used GAMs because they allow flexible modeling of nonlinear relationships while retaining interpretability due to their parametric components and smoothing functions (Hastie and Tibshirani, 1986; Yee and Mitchell, 1991).

Generalized additive models were fitted, including linear and nonlinear predictors, to identify factors affecting the iWUE. Tree age was modeled using a regression spline to account for possible ontogenetic nonlinearity, while climatic variables and CO_2 were used as linear terms. The tree species (SPEC) and site (SITE) were treated as categorical predictors. To test whether the species differ in the sensitivity to CO_2, we also included a $CO_2 \times$ SPEC interaction. The final model was the following (Equation 3):

$$\mathrm{iWUE} \sim s\left(\mathrm{AGE}, k=5\right) + \mathrm{VPD} + \mathrm{WB12} + \mathrm{CO_2} \times \mathrm{SPEC} + \mathrm{SITE} \quad (3)$$

To examine how variation in iWUE affects radial growth, we fitted a second GAM where the log-transformed BAI was the response variable. This model contained the same predictors as the iWUE model, but the iWUE was included as a species-specific smoothing function. This allowed the iWUE-growth relationship to vary among the species. The restriction to $k = 3$ was intentional to avoid biologically unrealistic, oscillating curves that may arise when higher-order polynomials are used. The final BAI model was the following (Equation 4):

$$\log\left(\mathrm{BAI}\right) \sim \mathrm{SPEC} + s\left(\mathrm{AGE}, k=10\right) + \mathrm{VPD} + \mathrm{WB12} + s\left(\mathrm{iWUE}, \mathrm{by}=\mathrm{SPEC}, k=3\right) + \mathrm{SITE} \quad (4)$$

For both modeling approaches, we started with a biologically relevant base model and tested additional terms (including interactions) sequentially. Model selection followed standard GAM procedures, relying on AIC, explained deviance and estimated degrees of freedom (EDF) to control model complexity and avoid overfitting (Burnham and Anderson, 2002; Wood, 2017). Model diagnostics confirmed that the selected models were stable and suitable for the assumptions of GAMs. GAM modeling was done using the mgcv package (v1.9–4; Wood, 2011). All statistical analyses were performed using R version 4.5.2 (R Core Team, 2026). Results were considered statistically significant when $p < 0.05$.

3 Results

3.1 Patterns of climate, $\Delta^{13}C$, $\delta^{18}O$, iWUE and BAI

Over the recent decades, mean annual temperature has increased significantly (Kendall's $\tau = 0.48–0.49$, $p < 0.05$), particularly after 1990, while total annual precipitation has shown no marked long-term change at both sites (Figure 2). The 12-month water balance (WB12) exhibited large interannual fluctuations but without a clear trend during the study period. In contrast, VPD has increased significantly (Kendall's $\tau = 0.39–0.50$, $p < 0.05$) over the past decades (Figure 2). The comparison of AET, used as a proxy for site-level microclimatic conditions indicated that the average summer AET during a severe drought period between 2000 and 2003 was around 10% higher at the GOD site and in its neighborhood (105 mm) than at the SOM site (96 mm).

Mean BAI was highest for *Q. cerris* and *T. tomentosa* at the SOM site, whereas among the GOD species only *F. ornus* reached similarly high values, as confirmed by the *t*-tests. The lowest average growth was observed in *A. campestre* at the GOD site, while the highest was recorded for *T. tomentosa* at the SOM site (Table 1). Tree species at the GOD site generally showed a continuous, but gradually slowing growth as they reached older age classes. In the case of *F. ornus*, however, a more pronounced decline in growth can be observed over the last two decades. In contrast, trees at the SOM site are younger (42–47 years), and therefore their growth was initially strong due to their age, but in recent decades a marked decline has occurred in *T. tomentosa* (Figure 3). As a result, the growth of *F. ornus* at the GOD site and *T. tomentosa* at the SOM site did not show a consistently increasing growth trend over their analyzed periods.

The $\Delta^{13}C$ values were similar among the species, except for *Q. cerris*, which showed significantly higher values than the other species at both study sites. According to the Mann–Kendall test, the carbon discrimination ($\Delta^{13}C$) trends during the past decades showed only a significant upward trend for *Q. cerris* at the GOD site. The $\delta^{18}O$ values were balanced among the analyzed species. Yet, no significant

10.3389/ffgc.2026.1922886

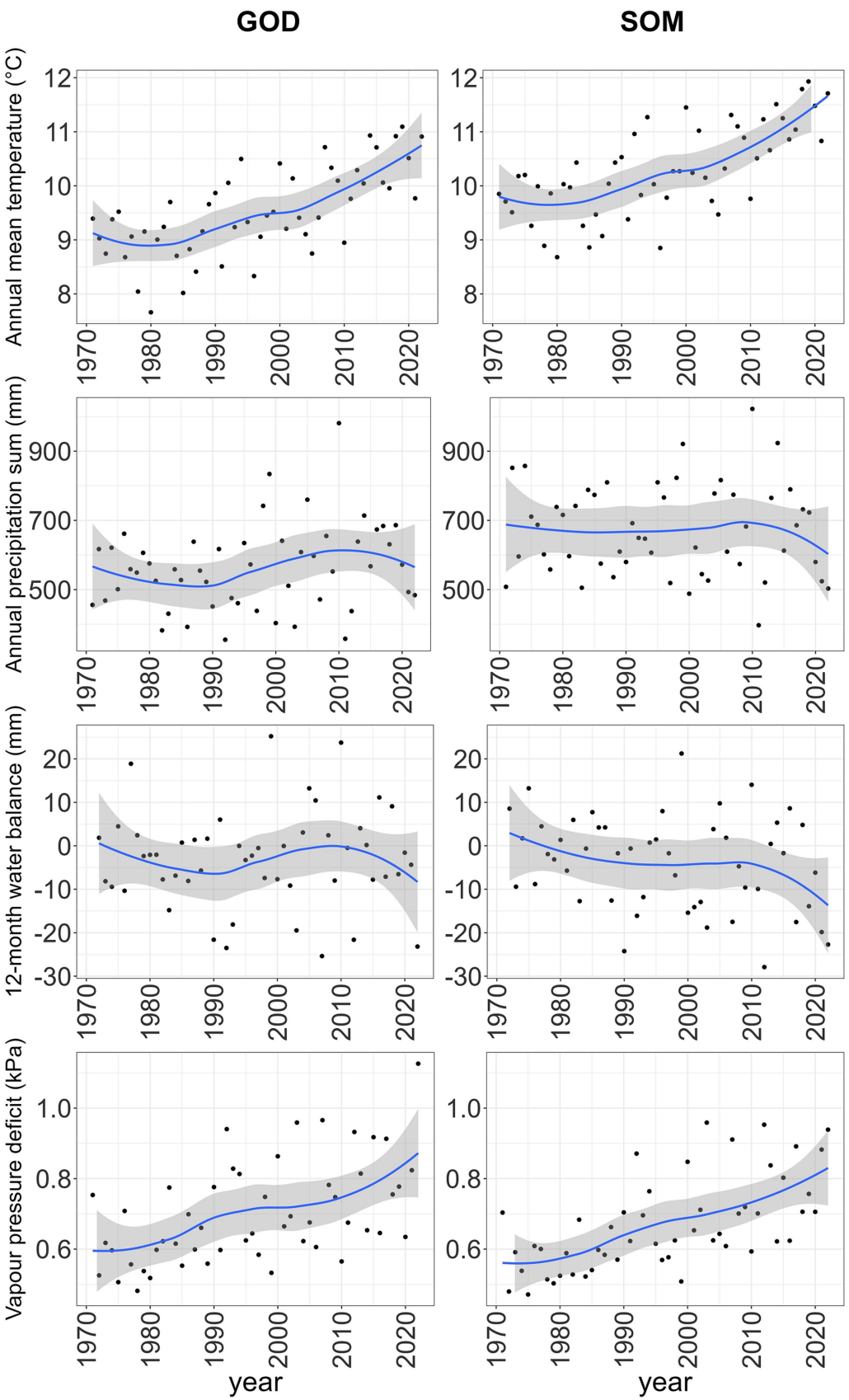

FIGURE 2
Trends of annual mean temperature (January–December), annual precipitation sum (January–December), 12-month water balance (between previous year September and actual year August) and vapor pressure deficit (summer months: June–August) in Gödöllő (GOD) and in Somogy Hills (SOM) sites.

10.3389/ffgc.2026.1922886

TABLE 1 Descriptive statistics of tree-ring variables for all species and sites.

Site	Species	Variables	Minimum	Maximum	Mean ± SE	SD
GOD	*A. campestre*	BAI (mm^2 $year^{-1}$)	139	1,284	614 ± 45	296
		$\Delta^{13}C$ (‰)	14.3	18.1	16.2 ± 0.12	0.8
		$\delta^{18}O$ (‰)	28.0	31.4	29.8 ± 0.10	0.7
		iWUE (μmol mol^{-1})	90.0	144.3	110.2 ± 1.70	11.5
	F. ornus	BAI (mm^2 $year^{-1}$)	336	2,508	1,006 ± 56	401
		$\Delta^{13}C$ (‰)	13.4	17.6	15.8 ± 0.12	0.9
		$\delta^{18}O$ (‰)	27.5	31.8	29.6 ± 0.14	1.0
		iWUE (μmol mol^{-1})	88.3	147.5	114.3 ± 1.91	13.8
	Q. cerris	BAI (mm^2 $year^{-1}$)	255	1,310	689 ± 31	222
		$\Delta^{13}C$ (‰)	15.1	19.3	16.9 ± 0.13	1.0
		$\delta^{18}O$ (‰)	27.1	30.2	28.9 ± 0.08	0.6
		iWUE (μmol mol^{-1})	77.6	129.6	101.4 ± 1.34	9.7
	Q. pubescens	BAI (mm^2 $year^{-1}$)	243	1803	875 ± 48	334
		$\Delta^{13}C$ (‰)	14.6	18.2	16.4 ± 0.13	0.9
		$\delta^{18}O$ (‰)	26.7	31.5	29.1 ± 0.11	0.8
		iWUE (μmol mol^{-1})	79.7	134.6	106.1 ± 1.69	12.2
SOM	*Q. cerris*	BAI (mm^2 $year^{-1}$)	201	3,191	1,185 ± 102	710
		$\Delta^{13}C$ (‰)	16.0	20.0	17.9 ± 0.14	1.0
		$\delta^{18}O$ (‰)	27.6	32.0	29.8 ± 0.15	1.1
		iWUE (μmol mol^{-1})	71.9	122.3	91.7 ± 1.61	11.6
	T. tomentosa	BAI (mm^2 $year^{-1}$)	351	3,068	1,201 ± 109	734
		$\Delta^{13}C$ (‰)	14.1	17.7	15.8 ± 0.11	0.8
		$\delta^{18}O$ (‰)	28.6	33.1	30.6 ± 0.14	1.0
		iWUE (μmol mol^{-1})	85.2	138.0	113.0 ± 1.61	11.6

Minimum, maximum, mean ± standard error (SE), and standard deviation (SD) are shown for basal area increment (BAI), carbon isotope discrimination ($\Delta^{13}C$), oxygen isotope composition ($\delta^{18}O$), and intrinsic water-use efficiency (iWUE) calculated from annual tree-ring records. Growth chronologies were based on 5 trees per species, while isotope chronologies were obtained from annual pooled samples of the same trees.

trends were found at the GOD site in the latewood $\delta^{18}O$ values for the species, except *Q. cerris*, which had a significant decreasing trend, whereas at the SOM site, $\delta^{18}O$ values increased significantly for both species. The mean iWUE of *Q. cerris* was lower than that of the other species at both sites (Table 1). The iWUE increased significantly over the study period at both sites and for all species. However, clear species-specific differences were observed. In *Q. cerris*, iWUE showed stagnation or only a slight increase until around 2010, followed by a modest increase thereafter (Sen's slope: 0.21 $year^{-1}$ at GOD and 0.29 $year^{-1}$ at SOM). In contrast, the other species exhibited a more consistent and steady increase in iWUE. The strongest increases were observed in *A. campestre* (Sen's slope: 0.64 $year^{-1}$) and *F. ornus* (Sen's slope: 0.63 $year^{-1}$) (Figure 3).

The $\delta^{18}O$ responses of the analyzed species showed marked differences to climatic extremes (Figure 4). At the GOD site, *F. ornus* revealed a pronounced increase in $\delta^{18}O$ data in the drought years compared to wet years. In contrast, *Q. cerris* and *A. campestre* showed much more restrained $\delta^{18}O$ changes during drought years as well as in wet years. *Q. pubescens* showed an intermediate pattern with moderate $\delta^{18}O$ fluctuations under variable climatic conditions. At the SOM site, where AET indicated drier surrounding conditions, *Q. cerris* demonstrated an entirely different pattern with a clear increase of $\delta^{18}O$ values in drought years and strongly negative $\delta^{18}O$ anomalies in wet years. *T. tomentosa* behaved similarly but with a larger spread of $\delta^{18}O$ values, indicating a more variable isotopic response to contrasting climatic conditions.

3.2 Relations of $\Delta^{13}C$, $\delta^{18}O$ and iWUE with climate variables

The correlation analysis revealed that the relationship among the climatic variables and isotope data were species and site specific (Figure 5A). $\Delta^{13}C$ showed consistently positive correlation with spring and summer precipitation (r = 0.25–0.5), though these relations were weaker at the SOM site. The effect of temperature was generally weaker, except for *A. campestre* and *F. ornus*, where $\Delta^{13}C$ was negatively correlated to the actual year summer temperature. The WB of the May–August period showed moderate correlation with $\Delta^{13}C$ (r up to 0.5), while the strongest relationship was observed for WB12 (r = 0.55–0.73) except for *A. campestre*, where the actual year summer water balance was more influential.

$\delta^{18}O$ data exhibited stronger and more consistent correlations at the SOM site. Notably, *Q. cerris* showed no significant relationships at the GOD site, but moderate correlations with summer climate variables at SOM (Figure 5B). A similar pattern was observed for *T. tomentosa*. At GOD, $\delta^{18}O$ data in *A. campestre*, *F. ornus* and *Q. pubescens* was

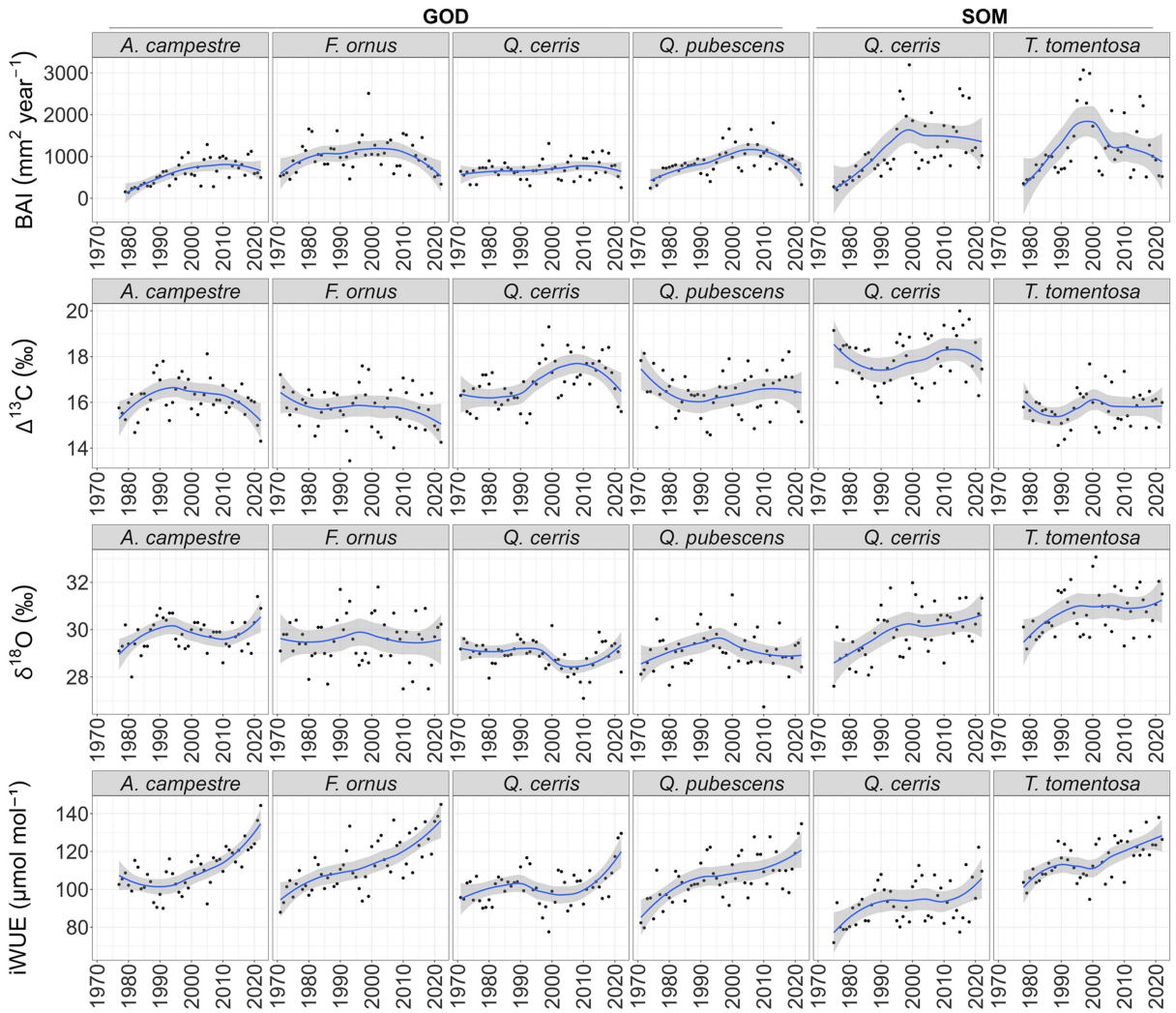

FIGURE 3
Temporal variation of basal area increment (BAI), $\Delta^{13}C$, $\delta^{18}O$ and iWUE of the analyzed broadleaf species at the sites GOD and SOM with loess regressions (blue lines) and 95% confidence intervals (gray shaded areas) with a span value of 1. Gödöllő Hills, GOD; Somogy Hills, SOM.

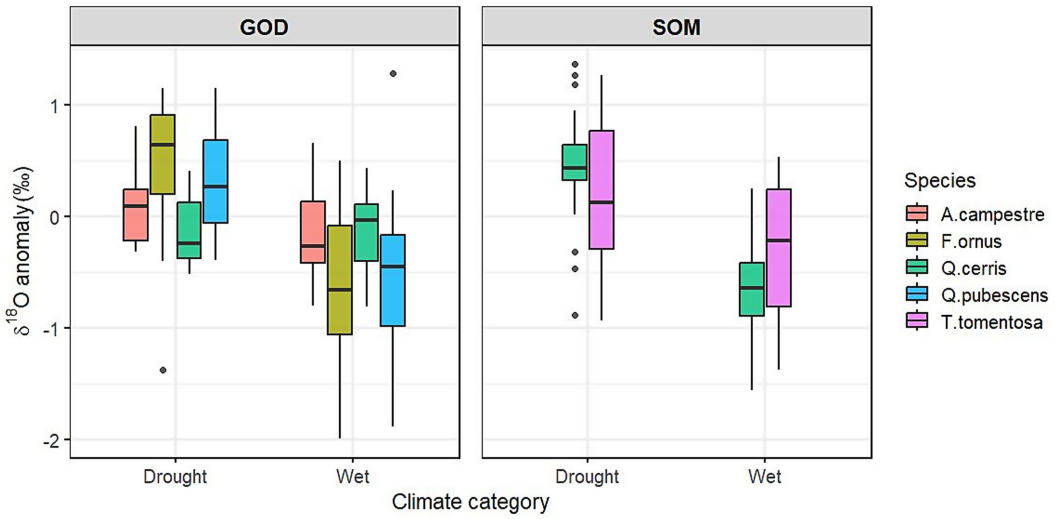

FIGURE 4
Species-specific $\delta^{18}O$ anomalies during drought and wet years at the sites GOD and SOM. Thick lines show the medians, the upper and lower box edges correspond to the first and third quartiles, whiskers extend to the most extreme values within 1.5 × the interquartile range, and circles indicate outliers. Gödöllő Hills, GOD; Somogy Hills, SOM.

10.3389/ffgc.2026.1922886

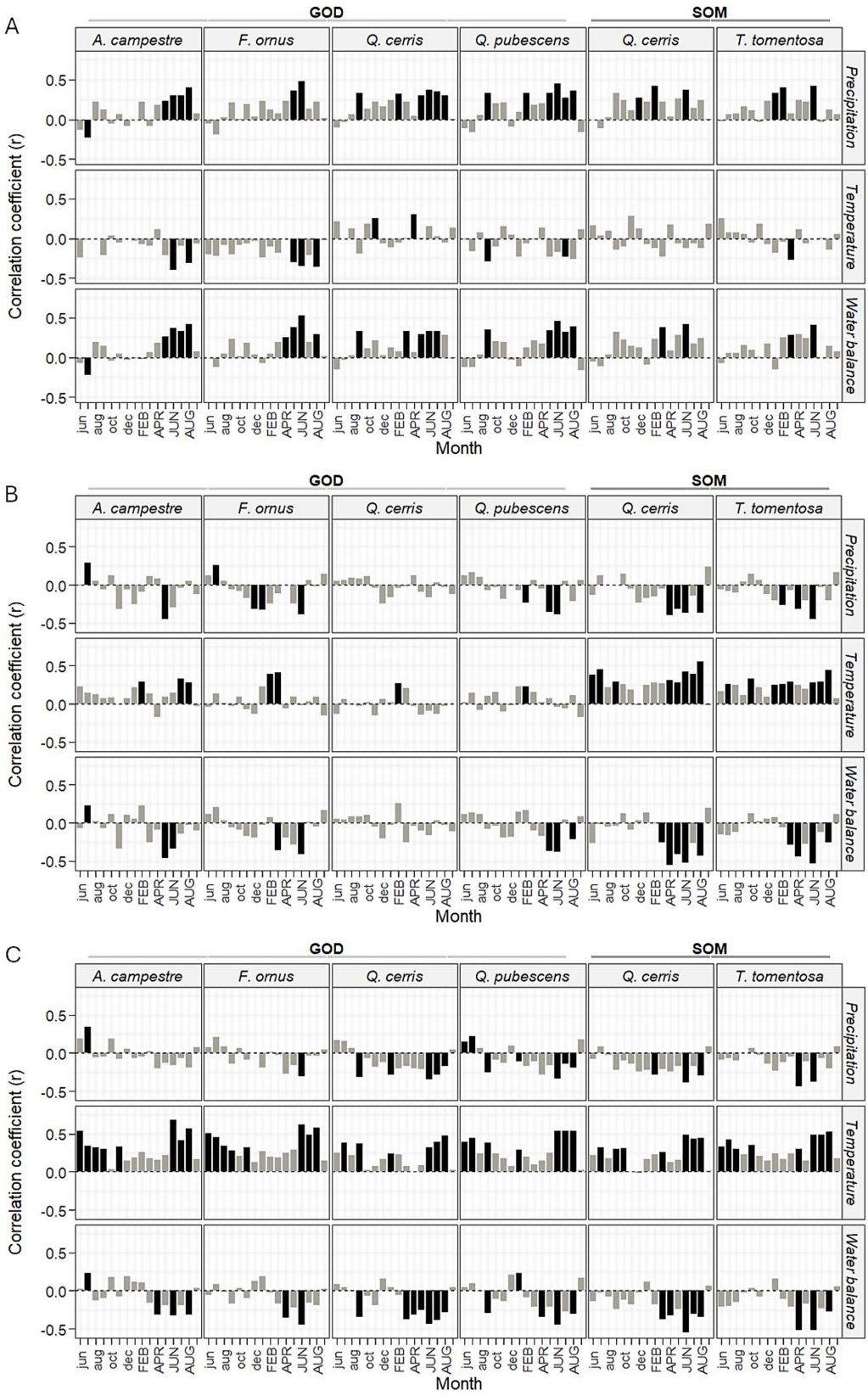

FIGURE 5
Pearson's correlations between monthly climate parameters and **(A)** $\Delta^{13}C$, **(B)** $\delta^{18}O$, and **(C)** iWUE for five native broadleaf tree species in the drier regions of East Central Europe. Lowercase month labels denote the previous growing year, whereas uppercase month labels denote the current growing year. Significant correlations ($p < 0.05$) are shown with black bars. Gödöllő Hills, GOD; Somogy Hills, SOM.

10.3389/ffgc.2026.1922886

mainly related to early growing-season precipitation and water balance, while February–March temperature had a positive effect in *F. ornus*. More pronounced relationships with cumulative water balance were observed only at SOM, particularly for *Q. cerris* ($r = -0.76$) and *T. tomentosa* ($r = -0.58$).

In contrast, iWUE showed a relative consistent pattern among the species and sites, with negative correlation with summer water balance and precipitation and positive correlation with summer temperature (r up to 0.62) (Figure 5C). The strongest relationship were detected for WB12 in the case of *Q. cerris* ($r = -0.69$ to -0.80) and *Q. pubescens* ($r = -0.60$). *F. ornus* and *A. campestre* were more strongly related to shorter seasonal water balance periods. VPD was also strongly correlated with iWUE across all species ($r = 0.64$ to 0.75).

Overall, the relationship of $\Delta^{13}C$ and $\delta^{18}O$ data showed negative correlations. At the GOD site, *A. campestre* and *Q. cerris* exhibited only weak negative relationships between $\Delta^{13}C$ and $\delta^{18}O$ ($r = -0.25$ to -0.23). Moderate correlations were found for *Q. pubescens* at the GOD site and for *Q. cerris* at the SOM site ($r = -0.47$ to -0.46). The strongest associations were observed for *F. ornus* at the GOD site and for *T. tomentosa* at the SOM site ($r = -0.63$ to -0.57).

3.3 Drivers of iWUE and its effects on tree growth across species

The model analyzing the environmental and physiological drivers of iWUE explained a substantial proportion of the variation in iWUE, with an adjusted R^2 of 0.77 and 78% deviance explained. The iWUE was significantly influenced by climatic water availability, atmospheric CO_2 concentration, and species identity, while tree age contributed a modest but significant nonlinear effect (Supplementary material 2). WB12 showed a strong negative linear effect, indicating that drier conditions were consistently associated with higher iWUE. VPD had a weaker, marginally significant positive effect. Atmospheric CO_2 had a clear positive effect on iWUE across species, but the magnitude of this response differed among species, as indicated by the significant $CO_2 \times$ SPEC interaction. The reference CO_2 sensitivity was strongly positive, and species-specific slopes revealed slight deviations from this trend (Figure 6).

Q. cerris exhibited a significantly weaker CO_2 response compared to the reference species (*A. campestre*), while *F. ornus* showed a slightly stronger, though only marginally significant, increase in iWUE with rising CO_2. *Q. pubescens* and *T. tomentosa* displayed CO_2 sensitivities similar to the reference level. Site effects were also significant (Supplementary material 2).

We fitted another model to examine the drivers of tree growth, expressed as log-transformed BAI. The model explained a substantial proportion of the variance (adjusted $R^2 = 0.75$, deviance explained = 76.6%), indicating a strong overall fit. Tree age showed a highly significant nonlinear effect on growth (edf ≈ 5.4, $p < 0.001$), reflecting complex ontogenetic trends. Among the climatic variables, VPD had a significant negative effect on growth, while water availability (WB12) had a positive effect, suggesting that water limitation constrains BAI. Species identity also influenced growth, with *Q. cerris* exhibiting significantly lower growth compared to the reference species, while other species showed no significant differences (Supplementary material 2).

Importantly, the relationship between iWUE and growth was species-specific (Figure 7). The smooth terms for iWUE were significant for all species, with mostly linear responses (edf ≈ 1), but with some indication of weak nonlinearity in certain species (e.g., *Q. cerris* and *T. tomentosa*). This indicates that changes in iWUE are consistently associated with growth, but the strength and shape of this relationship differ among species. Model diagnostics (k-index and edf values) confirmed that the chosen basis dimensions were adequate and that the model was not overfitted (Supplementary material 2). The partial effect curves indicate contrasting species-specific growth

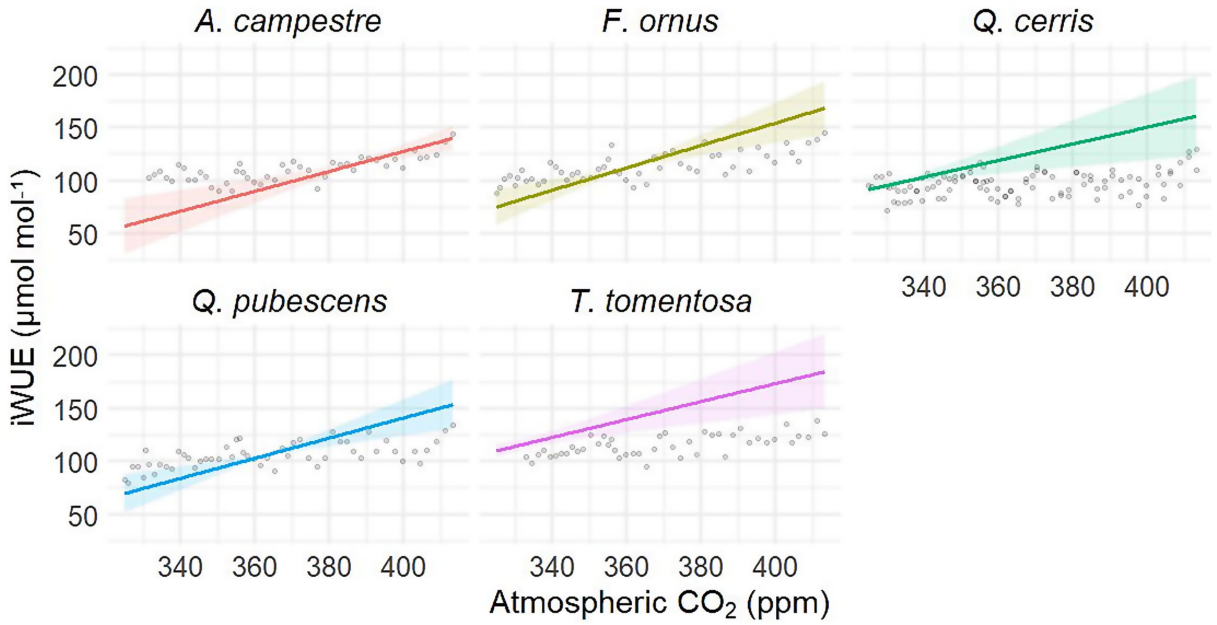

FIGURE 6
Species-specific *iWUE* response to atmospheric CO_2 changes (linear interaction model) for five native broadleaf tree species in the drier regions of East Central Europe. Points represent observed *iWUE* values, lines indicate model-predicted responses, and shaded areas denote the 95% confidence intervals.

10.3389/ffgc.2026.1922886

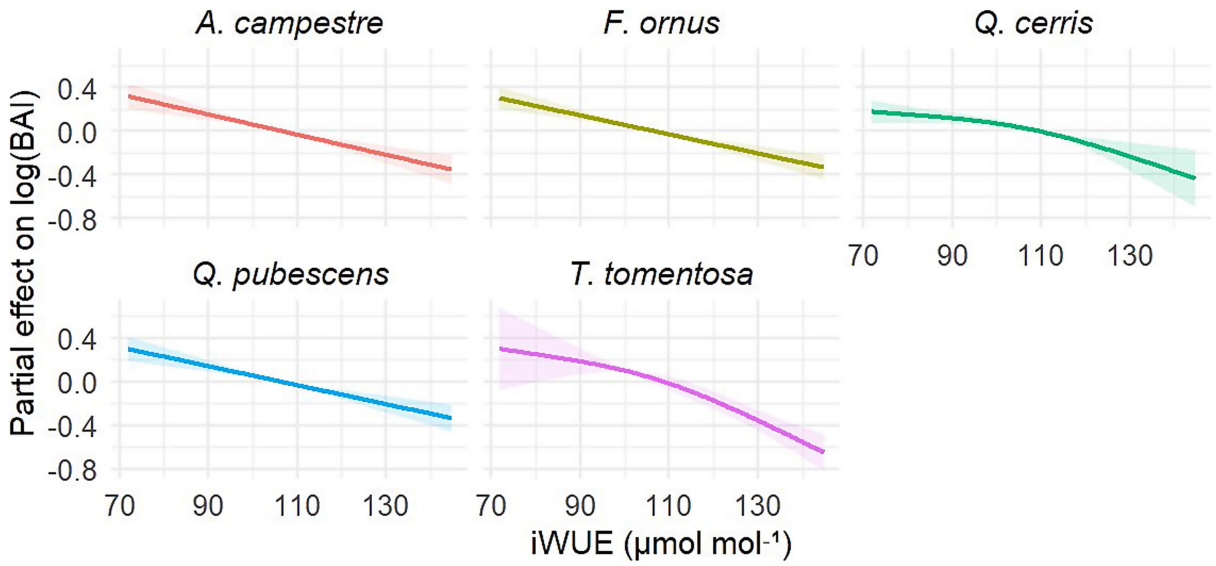

FIGURE 7
Species-specific growth response to iWUE changes (partial effect by species) for five native broadleaf tree species in the drier regions of East Central Europe. Shaded areas denote the 95% confidence intervals.

responses to increasing iWUE (Figure 7). In *T. tomentosa*, growth declines markedly with increasing iWUE, while *Q. cerris* shows a weaker response at lower iWUE values, followed by a sharper decline at higher iWUE, albeit with greater uncertainty (Figure 7).

4 Discussion

4.1 Temporal changes of $\Delta^{13}C$, $\delta^{18}O$ and iWUE and relations with climatic variables

The stable or increasing trend in $\Delta^{13}C$ data indicates that the physiological discrimination signal remained constant or strengthened, meaning that the residual variability mainly captures tree-level responses to water availability and evaporative conditions. The strong positive correlations between $\Delta^{13}C$ and summer climate variables (Figure 5A) – particularly at the site GOD – imply that the stomatal conductance was one of the decisive drivers of carbon isotope discrimination and that the stomatal regulation played a key role in the preservation of leaf water status during dry conditions (Farquhar et al., 1989).

The distinct trends of $\delta^{18}O$ values – decreasing or stable at GOD and increasing at SOM (Figure 3) – emphasize further the role of eco-hydrological conditions in shaping the leaf-level evaporative processes. At SOM, $\delta^{18}O$ showed stronger and more consistent correlations with summer temperature, precipitation and water balance. This suggests that the evaporative enrichment of leaf water was strongly coupled to atmospheric dryness. In contrast, at the site GOD, the $\delta^{18}O$ data showed weaker correlation that may imply access to deeper soil moisture or species-specific differences in leaf water turnover.

The contrasting behavior of the two isotopes does not represent a contradiction, but it may reflect their sensitivity to different components of drought stress. While $\Delta^{13}C$ responds primarily to stomatal regulation driven by soil moisture deficit (Eilmann et al., 2010), $\delta^{18}O$ signal integrates several interacting processes, including the isotopic composition of source water, leaf-water evaporative enrichment and atmospheric humidity (Dongmann et al., 1974; Farquhar and Lloyd, 1993; Sternberg, 2009). This is also consistent with recent syntheses highlighting the multiple controls on tree-ring $\delta^{18}O$ under drought conditions (Bailey et al., 2025). Accordingly, $\Delta^{13}C$ showed a more clear signal at GOD, whereas $\delta^{18}O$ signal reflects a stronger relationship to atmospheric stress at SOM. This difference may reflect the contrasting microclimatic conditions of the sites. While GOD is situated within a larger and more continuous forested area, SOM is surrounded by agricultural land within a relatively short distance (Figure 1). The larger forest area surrounding GOD likely buffers local microclimatic extremes by maintaining a more humid atmosphere and reducing atmospheric mixing. Consequently, trees at GOD may experience lower evaporative demand even during drought periods. As a result, atmospheric drought stress may be partly moderated even during droughts. On the other hand, SOM is surrounded by scattered landscape and therefore more exposed to warm and dry air originating from adjacent open areas that may lead to higher evaporative demand and stronger leaf-water enrichment. More generally, these findings suggest that tree responses to drought are influenced not only by macroclimatic conditions but also by the surrounding landscape and its effects on local microclimatic conditions. Supporting this interpretation, actual evapotranspiration during the severe drought period (2000–2003) was approximately 10% higher at GOD than at SOM. Although AET does not directly measure microclimate, this difference is consistent with a greater capacity of the larger forested landscape to buffer local drought conditions. An alternative explanation could be differences in the isotopic composition of source water between sites or among years. However, both study sites lack access to groundwater and are primarily supplied by precipitation. Given the relatively short distance (ca. 110 km) and similar elevation of the two study sites (Figure 1), major differences in precipitation $\delta^{18}O$ values cannot be expected (Kern et al., 2020). Although this possibility cannot be entirely excluded without direct measurements of precipitation and soil-water isotopic composition, we consider differences in

evaporative enrichment associated with site-specific microclimatic conditions to be the more likely explanation. Because only two sites were compared, the proposed role of landscape-mediated microclimatic buffering should be regarded as a plausible interpretation rather than direct experimental evidence.

The iWUE has been significantly increased for all species at both sites, especially after 2010. This is in line with global observations, according to which the iWUE is increasing globally as a response to the rising atmospheric CO_2 concentration (Saurer et al., 2004; Mathias and Thomas, 2021). At the same time, the magnitude of increase is considerably variable among tree species, which reflects different physiological strategies. *Q. cerris* exhibited a characteristically water-spending strategy with relatively low iWUE in both stands (Figure 3) and more open stomata during most of the study period. This strategy supports the continuous carbon assimilation and growth at a favorable water supply. After 2010, when the drought frequency and VPD have been increased (Figure 2), *Q. cerris* shifted to a more conservative water use strategy, which was consistent with the sharp rise in iWUE and stronger stomatal regulation. Several dendrochronological studies have confirmed the high growth sensitivity of *Q. cerris* to drought (Móricz et al., 2021; Kostić et al., 2022; Mészáros et al., 2022). In contrast, *A. campestre* and *F. ornus* revealed a more gradual and more consistent increase in iWUE, implying earlier or more sensitive response to the increasingly drying conditions at the stomatal level. Our previous analysis in the study area pointed to interspecific differences: *A. campestre*, *F. ornus* and *T. tomentosa* showed greater variability and sensitivity to drought, while *Q. cerris* and *Q. pubescens* have outstanding resilience and maintain stable growth even under drier conditions (Móricz et al., 2025). This is partly consistent with the current results but also suggests that drought responses of the species strongly depend on site-specific water availability and microclimatic conditions.

The $\delta^{18}O$ patterns showed clear species- and site-specific differences in how the trees reacted to distinct climatic conditions. At the GOD site, *F. ornus* revealed the highest isotopic sensitivity, with pronounced increases in $\delta^{18}O$ values during drought years and significant decreases in wet years (Figure 4). This pattern is consistent with higher evaporative demand and greater drought sensitivity of this species. In contrast, *Q. cerris* and *A. campestre* showed more balanced responses, with no significant $\delta^{18}O$ fluctuations between drought and wet years, suggesting more conservative leaf-water isotopic behavior or the use of deeper soil water sources. *Q. pubescens* occupied an intermediate position, showing moderate increases and decreases in $\delta^{18}O$ values during drought and wet years, respectively (Figure 4), indicating a balanced response. At the SOM site, *Q. cerris* displayed a contrasting pattern compared to the site GOD. In drought years, clear $\delta^{18}O$ increase was observed, while in wet years, strong negative values were observed (Figure 4), consistent with the site-specific $\delta^{18}O$-climate relationships. The pattern of *T. tomentosa* was similar to *Q. cerris* at SOM, but with greater variability (Figure 4), indicating a more inconsistent isotopic response to changing moisture conditions. The observed species-specific differences agree with previous studies showing that tree-ring $\delta^{18}O$ integrates differences in stomatal regulation, transpiration and source-water use among species under contrasting moisture conditions (Barbour, 2007).

The strong relationship between iWUE and climatic variables (especially water balance and summer VPD, see Figure 5C) suggest that the growing evaporative demand increasingly limits the stomatal conductance, leading to higher iWUE. This is in line with the concept that the higher iWUE during drought is mainly consistent with increased stomatal limitation. The temporal alignment of isotopic and growth patterns provides insight into the species-specific drought responses. For several species, the iWUE has risen steeply after 2010, coincident with the period of frequent and severe droughts, while growth was stagnant or decreased (Figure 3). This decoupling of iWUE and growth indicate that the higher iWUE does not necesseraly translate into higher carbon gain or productivity under water-limited conditions (Peñuelas et al., 2011; Lévesque et al., 2014; Fajardo et al., 2019; Assefa et al., 2025). Instead, it likely consistent with a conservative water use strategy, where stomatal closure maintains leaf water status at the expense of carbon assimilation. Such patterns have been reported in numerous studies and are often interpreted as early warning signals of increasing drought stress and potential future growth decline (Timofeeva et al., 2017; Peters et al., 2018; Kannenberg et al., 2021).

The strong negative correlations between $\Delta^{13}C$ and $\delta^{18}O$ data observed in *F. ornus* and *T. tomentosa* suggest a tight coupling between stomatal regulation and leaf water evaporative enrichment. This suggests that stomatal regulation and leaf-water enrichment were tightly coupled under changing atmospheric demand. In contrast, the weaker relationships found for *A. campestre* and *Q. cerris* at the GOD site suggest a partial decoupling between stomatal conductance and leaf water enrichment. This implies a greater influence of non-stomatal (biochemical) limitations on $\Delta^{13}C$, and less pronounced stomatal restriction during the growing season. Notably, the correlation for *Q. cerris* at the SOM site was substantially stronger than at the GOD site. This pattern is consistent with a stronger atmospheric control on gas exchange under the more exposed microclimatic conditions at SOM. Overall, it supports the presence of site-specific differences in drought-related physiological regulation between the two locations.

4.2 Species-specific drivers of iWUE and its effects on tree growth

The GAM modeling provided insights into how the climatic variables, the atmospheric CO_2 and species characteristics shape the iWUE jointly and how these changes influence the radial growth of trees. The iWUE model had high explanatory power, which highlighted the marked and well-predictable effect of water supply and CO_2 concentration (Supplementary material 2). The substantial effect of WB12 confirmed the soil water deficit as the main driver of iWUE increase in accordance with the mechanism of stomatal regulation under drought (Timofeeva et al., 2017). Although some studies emphasized the importance of the VPD effect on iWUE (e.g., Pernicová et al., 2024), our results revealed only a slight effect of VPD. The significant CO_2 × species interaction (Figure 6) indicated that the increase in iWUE associated with rising atmospheric CO_2 differed among species. These differences likely reflect the distinct hydraulic architecture, stomatal sensitivity and photosynthetic capacity of species.

The growth model showed that the main determinants of BAI were tree age, water supply and VPD in accordance with the known ontogenetic and climatic factors regulating growth (Supplementary material 2). Importantly, the smoothing functions of species-specific iWUE showed that the relationship of water use efficiency and growth is not uniform among the species (Figure 7). For example, the growth of *T. tomentosa* declined steeply with increasing iWUE, which indicated a strong trade-off between

water conservation and carbon assimilation. This suggest that the stomatal closure during drought events limits photosynthesis, leading to reduced growth despite higher iWUE. In contrast, *Q. cerris* showed a nonlinear response with relatively stable growth at low to moderate iWUE but a sharp drop in growth at higher iWUE values. It may refer to a threshold, above which the stomatal regulation becomes too restricitive for carbon assimilation. These findings align with broader evidence that rising atmospheric CO_2 does not uniformly enhance tree growth, particularly in water-limited environments (Peñuelas et al., 2011; Granda et al., 2014; Lévesque et al., 2014; Zhang et al., 2025). Recent work on sessile oak similarly demonstrated that site conditions and tree characteristics strongly modulate iWUE responses to drought, highlighting substantial within-species variability (Meeran et al., 2025). Collectively, these studies indicate that the interaction between CO_2 fertilization and drought determines whether increases in iWUE translate into productivity gains or merely reflect stress-induced stomatal closure. The species-specific responses observed here underscore the importance of considering functional traits, rooting depth, and hydraulic strategies when predicting forest responses to future climate change.

4.3 Limitations

This study has several limitations that should be considered when interpreting the results. First, isotope analysis was performed on pooled samples from five trees per species and not on individual trees. Although this approach is widely used in the tree-ring isotope research and provides robust stand-level signal (Leavitt, 2010; Loader et al., 2013), it does not allow the analysis of within-species variability or individual tree responses (Belmecheri et al., 2022). Furthermore, we examined only two sites at the drought-prone region of Central Hungary. Therefore, our results should be representative mainly in the drier and drought-prone regions of East-Central Europe, not for the whole region. The differences in tree age among species and sites may influence the observed changes in growth and physiological responses. Although, tree age was explicitly incorporated in the GAM models, the non-linear ontogenetical effects on hydraulic architecture and climate sensitivity cannot be separated entirely from the species-specific responses. The $\delta^{18}O$ signal is considered to be less sensitive to tree age than tree growth or carbon isotope signals that suggest that the identified main physiological patterns are not driven exclusively by ontogenetical effects (Duffy et al., 2019; Büntgen et al., 2020). The role of landscape mediated microclimatic buffering should be interpreted cautiously. However, the two study sites are climatically similar on a regional scale and they differ in the surrounding forest cover and actual evapotranspiration during drought years, but the direct within-stand microclimatic measurements (air temperature, relative humidity, soil moisture) were not available. For that reason, the effect of landscape structure on isotopic responses represents a probable interpretation that are supported by indirect evidence, and not direct experimental demonstration. Future studies that incorporate continuous microclimate monitoring at larger number of sites would allow the testing of this hypothesis. Since direct gas-exchange measurements were not available, the increase of iWUE cannot be attributed exclusively to reduced stomatal conductance. The observed patterns may reflect either the decrease of photosynthetic capacity or the stomatal conductance or both.

5 Conclusion

The long-term isotopic and growth analysis have shown that the studied five native broadleaf tree species are already under considerable climatic stress in the drier regions of East Central Europe due to rising temperatures and more frequent droughts. Although the water use efficiency has increased in the last few decades for all species, these changes were not accompanied by lasting and increased growth. This suggests that the higher atmospheric CO_2 did not compensate for the unfavorable effect of warming and drying. The species displayed variable drought response strategies. *T. tomentosa* and *F. ornus* employed a more conservative water use with sharply increasing iWUE; however, their growth has slowed significantly. This strategy may help with short-term survival but may lead to carbon depletion and increased vulnerability. In contrast, *Q. pubescens* and *A. campestre* were able to maintain their growth under increasing iWUE, suggesting that their hydraulic properties or rooting depth moderates the negative effect of droughts. *Q. cerris* showed an intermediate pattern with quasi-constant growth during even medium stress, while its growth declined significantly under severe drought. Beyond species-specific differences, our results suggest that site conditions and surrounding landscape structure may also influence drought responses through local microclimatic effects, although species identity remains the primary driver of the observed patterns. Together, these findings highlight strong interspecific differences in physiological and hydraulic drought-response strategies.

Data availability statement

The raw data supporting the conclusions of this article will be made available by the authors, without undue reservation.

Author contributions

NM: Conceptualization, Data curation, Funding acquisition, Investigation, Methodology, Project administration, Writing – original draft, Writing – review & editing. IM: Conceptualization, Funding acquisition, Methodology, Supervision, Writing – original draft, Writing – review & editing. ZK: Conceptualization, Data curation, Funding acquisition, Investigation, Methodology, Supervision, Writing – original draft, Writing – review & editing. GI: Data curation, Investigation, Supervision, Writing – original draft, Writing – review & editing. CE: Data curation, Formal analysis, Funding acquisition, Investigation, Methodology, Writing – original draft, Writing – review & editing. IB: Conceptualization, Investigation, Supervision, Writing – original draft, Writing – review & editing. TN: Conceptualization, Data curation, Formal analysis, Funding acquisition, Investigation, Methodology, Writing – original draft, Writing – review & editing.

Funding

The author(s) declared that financial support was received for this work and/or its publication. Project no. FK 142468 has been implemented with the support provided by the Ministry of Culture and Innovation of Hungary from the National Research, Development and Innovation Fund, financed under the FK_22 "OTKA" young researchers' excellence programme funding scheme.

Acknowledgments

The authors express their gratitude to the local state forest companies (SEFAG Ltd., branch office Szántód; Pilisi Parkerdő Ltd., branch office Gödöllő) for their valuable support in the field. The authors are thankful to István Hegyi (Budapest) for his work in the isotopic laboratory. The laboratory of the Forest Research Institute is also acknowledged for the soil analysis. In addition, our colleagues are thanked for their help with the fieldwork and assistance. Lastly, we also grateful to the reviewers for their valuable and constructive criticism.

Conflict of interest

The author(s) declared that this work was conducted in the absence of any commercial or financial relationships that could be construed as a potential conflict of interest.

The author IM declared that they were an editorial board member of Frontiers, at the time of submission. This had no impact on the peer review process and the final decision.

Generative AI statement

The author(s) declared that Generative AI was used in the creation of this manuscript. Artificial intelligence (ChatGPT, OpenAI) was used to assist with language editing and improvement of the manuscript text.

Any alternative text (alt text) provided alongside figures in this article has been generated by Frontiers with the support of artificial intelligence and reasonable efforts have been made to ensure accuracy, including review by the authors wherever possible. If you identify any issues, please contact us.

Publisher's note

Supplementary material

The Supplementary material for this article can be found online at: https://www.frontiersin.org/articles/10.3389/ffgc.2026.1922886/full#supplementary-material

References

Ainsworth, E. A., and Rogers, A. (2007). The response of photosynthesis and stomatal conductance to rising [CO2]: mechanisms and environmental interactions. *Plant Cell Environ.* 30, 258–270. doi: 10.1111/j.1365-3040.2007.01641.x

Andreu-Hayles, L., Plannels, O., Gutiérrez, E., Muntan, E., Helle, G., Anchukaitis, K. J., et al. (2011). Long tree-ring chronologies reveal 20th century increases in water-use efficiency but no enhancement of tree growth at five Iberian pine forests. *Glob. Change Biol.* 17, 2095–2112. doi: 10.1111/j.1365-2486.2010.02373.x

Assefa, S., Ventura, M., Bravo, F., Giberti, G. S., Olivar, J., Bielak, K., et al. (2025). Pure and mixed Scots pine forests showed divergent responses to climate variation and increased intrinsic water use efficiency across a European-wide climate gradient. *Eur. J. Forest Res.* 144, 875–892. doi: 10.1007/s10342-024-01731-8

Bailey, K., Szejner, P., Strange, B., Nabours, R., Monson, R. K., and Hu, J. (2025). The aridity influence on oxygen isotopes recorded in tree rings. *Tree Physiol.* 45:tpaf044. doi: 10.1093/treephys/tpaf044

Barbour, M. M. (2007). Stable oxygen isotope composition of plant tissue: a review. *Funct. Plant Biol.* 34, 83–94. doi: 10.1071/FP06228

Belmecheri, S., Wright, W. E., and Szejner, P. (2022). Sample Collection and Preparation for Annual and Intra-annual Tree-Ring Isotope Chronologies. In: Siegwolf, R.T.W., Brooks, J.R., Roden, J., Saurer, M. (eds) Stable Isotopes in Tree Rings. *Tree Physiology* 8. Springer, Cham. doi: 10.1007/978-3-030-92698-4_4

Bosela, M., Tumajer, J., Cienciala, E., Dobor, L., Kulla, L., Marčiš, P., et al. (2021). Climate warming induced synchronous growth decline in Norway spruce populations across biogeographical gradients since 2000. *Sci. Total Environ.* 752:141794. doi: 10.1016/j.scitotenv.2020.141794

Büntgen, U., Kolář, T., Rybníček, M., Koňasová, E., Trnka, M., Ač, A., et al. (2020). No Age Trends in Oak Stable Isotopes. *Paleoceanography and Paleoclimatology.* 35: e2019PA003831. doi: 10.1029/2019PA003831

Burnham, K. P., and Anderson, D. R. (2002). *Model Selection and Multimodel Inference: A Practical Information-Theoretic Approach*. New York, NY: Springer.

Caudullo, G., and de Rigo, D. (2016). "*Fraxinus ornus* in Europe: distribution, habitat, usage and threats," in *European Atlas of Forest Tree Species*, eds. J. San-Miguel-Ayanz, D. Rigo, G. Caudullo, T. Houston Durrant and A. Mauri (Luxembourg: Publications Office of the European Union).

de Rigo, D., Enescu, C. M., Houston Durrant, T., and Caudullo, G. (2016). "*Quercus cerris* in Europe: distribution, habitat, usage and threats," in *European Atlas of Forest Tree Species*, eds. J. San-Miguel-Ayanz, D. Rigo, G. Caudullo, T. Houston Durrant and A. Mauri (Luxembourg: Publications Office of the European Union).

Dongmann, G., Nürnberg, H. W., Förstel, H., and Wagener, K. (1974). On the enrichment of $H_2{}^{18}O$ in the leaves of transpiring plants. *Radiat. Environ. Biophys.* 11, 41–52. doi: 10.1007/BF01323099

Dorado-Liñán, I., Valbuena-Carabana, M., Canellas, I., Gil, L., and Gea-Izquierdo, G. (2020). Climate change synchronizes growth and iWUE across species in a temperate submediterranean mixed oak forest. *Front. Plant Sci.* 11:706. doi: 10.3389/fpls.2020.00706

Duffy, J. E., McCarroll, D., Loader, N. J., Young, G. H. F., Davies, D., Miles, D., et al. (2019). Absence of age-related trends in stable oxygen isotope ratios from oak tree rings. *Glob. Biogeochem. Cycles* 33, 841–848. doi: 10.1029/2019GB006195

Eaton, E., Caudullo, G., and de Rigo, D. (2016). "*Tilia cordata*, Tilia platyphyllos and other limes in Europe: distribution, habitat, usage and threats," in *European Atlas of Forest Tree Species*, eds. J. San-Miguel-Ayanz, D. Rigo, G. Caudullo, T. Houston Durrant and A. Mauri (Luxembourg: Publications Office of the European Union).

Ehleringer, J. R., Hall, A. E., and Farquhar, G. D. (1993). "Introduction: water use in relation to productivity," in *Stable Isotopes and Plant Carbon-Water Relations*, eds. J. R. Ehleringer, A. E. Hall and G. D. Farquhar (New York: Academic Press), 3–8.

Eilmann, B., Buchmann, N., Siegwolf, R., Saurer, M., Cherubini, P., and Rigling, A. (2010). Fast response of Scots pine to improved water availability reflected in tree-ring width and d13C. *Plant Cell Environ.* 33, 1351–1360. doi: 10.1111/j.1365-3040.2010.02153.x

Enderle, L., Gribbe, S., Muffler, L., Weigel, R., Hertel, D., and Leuschner, C. (2024). A warmer climate impairs the growth performance of Central Europe's major timber species in lowland regions. *Sci. Total Environ.* 941:173665. doi: 10.1016/j.scitotenv.2024.173665

Fajardo, A., Gazol, A., Mayr, C., and Camarero, J. J. (2019). Recent decadal drought reverts warming triggeredgrowth enhancement in contrasting climates in the southern Andes tree line. *J. Biogeogr.* 46, 1367–1379. doi: 10.1111/jbi.13580

Farquhar, G. D., Ehleringer, J. R., and Hubick, K. T. (1989). Carbon isotope discrimination and photosynthesis. *Annu. Rev. Plant Physiol. Plant Mol. Biol.* 40, 503–537. doi: 10.1146/annurev.pp.40.060189.002443

Farquhar, G., O'Leary, M. H. O., and Berry, J. (1982). On the relationship between carbon isotope discrimination and the intercellular carbon dioxide concentration in leaves. *Australian journal of plant physiology.* 9, 121–137.

Farquhar, G. D., and Lloyd, J. (1993). "Carbon and oxygen isotope effects in the exchange of carbon dioxide between terrestrial plants and the atmosphere," in *Stable Isotopes and Plant Carbon–Water Relations*, eds. J. R. Ehleringer, A. E. Hall and G. D. Farquhar (San Diego, CA, USA: Academic Press), 47–70.

Frank, D. C., Poulter, B., Saurer, M., Esper, J., Huntingford, C., Helle, G., et al. (2015). Water-use efficiency and transpiration across European forests during the Anthropocene. *Nat. Clim. Chang.* 5, 579–583. doi: 10.1038/nclimate2614

Giammarchi, F., Cherubini, P., Pretzsch, H., and Tonon, G. (2017). The increase of atmospheric CO2 affects growth potential and intrinsic water-use efficiency of Norway spruce forests: insights from a multi-stable isotope analysis in tree rings of two alpine chronosequences. *Trees* 31, 503–515. doi: 10.1007/s00468-016-1478-2

Granda, E., Rossatto, D. R., Camarero, J. J., Voltas, J., and Valladares, F. (2014). Growth and carbon isotopes of Mediterranean trees reveal contrasting responses to increased carbon dioxide and drought. *Oecologia* 174, 307–317. doi: 10.1007/s00442-013-2742-4

Grossiord, C., Buckley, T. N., Cernusak, L. A., Novick, K. A., Poulter, B., Siegwolf, R. T., et al. (2020). Plant responses to rising vapor pressure deficit. *New Phytol.* 226, 1550–1566. doi: 10.1111/nph.16485

Guerrieri, R., Belmecheri, S., Ollinger, S. V., Asbjornsen, H., Jennings, K., Xiao, J., et al. (2019). Disentangling the role of photosynthesis and stomatal conductance on rising forest water-use efficiency. *Proc. Natl. Acad. Sci.* 116, 16909–16914. doi: 10.1073/pnas.1905912116

Hartl-Meier, C., Zang, C., Buentgen, U., Esper, J., Rothe, A., Goettlein, A., et al. (2015). Uniform climate sensitivity in tree-ring stable isotopes across species and sites in a mid-latitude temperate forest. *Tree Physiol.* 35, 4–15. doi: 10.1093/treephys/tpu096

Hastie, T., and Tibshirani, R. (1986). Generalized additive models. *Statist. Sci.* 1, 297–310.

Helle, G., Pauly, M., Heinrich, I., Schollän, K., Balanzategui, D., and Schürheck, L. (2022). "Stable Isotope Signatures of Wood, its Constituents and Methods of Cellulose Extraction," in *Stable Isotopes in Tree Rings Tree Physiology 8*, eds. R. T. W. Siegwolf, J. R. Brooks, J. Roden and M. Saurer (Cham: Springer).

Hereş, A.-M., Camarero, J. J., López, B. C., and Martínez-Vilalta, J. (2014). Declining hydraulic performances and low carbon investments in tree rings predate Scots pine drought-induced mortality. *Trees*. 1737–1750. doi: 10.1007/s00468-014-1081-3

HMS (2025) Meteorological database. Available online at: https://odp.met.hu/climate/homogenized_data/gridded_data_series/ (Accessed November 15, 2025).

Holmes, R. L. (1983). Computer-assisted quality control in tree-ring dating and measurement. *Tree-Ring Bull.* 43, 69–78.

Huang, J. G., Bergeron, Y., Denneler, B., Berninger, F., and Tardif, J. (2007). Response of Forest trees to increased atmospheric CO_2. *Crit. Rev. Plant Sci.* 26, 265–283. doi: 10.1080/07352680701626978

Kagawa, A., Sugimoto, A., and Maximov, T. C. (2006). $^{13}CO_2$ pulse-labelling of photoassimilates reveals carbon allocation within and between tree rings. *Plant Cell Environ.* 29, 1571–1584. doi: 10.1111/j.1365-3040.2006.01533.x

Kannenberg, S. A., Driscoll, A. W., Szejner, P., Anderegg, W. R. L., and Ehleringer, J. R. (2021). Rapid increases in shrubland and forest intrinsic water-use efficiency during an ongoing megadrought. *Proc. Natl. Acad. Sci. USA* 118:e2118052118. doi: 10.1073/pnas.2118052118

Keenan, T. F., Hollinger, D. Y., Bohrer, G., Dragoni, D., Munger, J. W., Schmid, H. P., et al. (2013). Increase in forest water-use efficiency as atmospheric carbon dioxide concentrations rise. *Nature* 499, 324–327. doi: 10.1038/nature12291

Kern, Z., Hatvani, I. G., Czuppon, G., Fórizs, I., Erdélyi, D., Kanduč, T., et al. (2020). Isotopic 'altitude' and 'continental' effects in modern precipitation across the Adriatic–Pannonian region. *Water* 12:1797. doi: 10.3390/w12061797

Kern, Z., Llanos Campana, D. M., and Hegyi, I. N. (2022). Long-term performance of simultaneous measurement of stable isotopes of oxygen and carbon in cellulose with a high-temperature pyrolysis/gas chromatography/isotope ratio mass spectrometry system at the Institute for Geological and Geochemical Research. *Cent. Eur. Geol.* 65, 137–143. doi: 10.1556/24.2023.00134

Kimak, A., and Leuenberger, M. (2015). Are carbohydrate storage strategies of trees traceable by earlylatewood carbon isotope differences? *Trees* 29, 859–870. doi: 10.1007/s00468-015-1167-6

Knutzen, F., Averbeck, P., Barrasso, C., Bouwer, L. M., Gardiner, B., Grünzweig, J. M., et al. (2025). Impacts on and damage to European forests from the 2018–2022 heat and drought events. *Nat. Hazards Earth Syst. Sci.* 25, 77–117. doi: 10.5194/nhess-25-77-2025

Kostić, S., Levanič, T., Orlović, S., Matović, B., and Stojanović, D. B. (2022). Turkey oak (*Quercus cerris* L.) is more drought tolerant and better reflects climate variations compared to pedunculate oak (*Quercus robur* L.) in lowland mixed forests in northwestern Serbia: a stable carbon isotope ratio (δ13C) and radial growth approach. *Ecol. Indic.* 142:109242. doi: 10.1016/j.ecolind.2022.109242

Laumer, W., Andreu, L., Helle, G., Schleser, G. H., Wieloch, T., and Wissel, H. (2009). A novel approach for the homogenization of cellulose to use micro-amounts for stable isotope analyses. *Rapid Commun. Mass Spectrom.* 23, 1934–1940. doi: 10.1002/rcm.4105

Leavitt, S. W. (2010). Tree-ring C-H-O isotope variability and sampling. *Sci. Total Environ.* 408, 5244–5253. doi: 10.1016/j.scitotenv.2010.07.057

Leuenberger, M. (2007). "To what extent can ice core data contribute to the understanding of plant ecological developments of the past?" in *Stable Isotopes as Indicators of Ecological Change, Terrestrial Ecology*, eds. T. E. Dawson and R. T. W. Siegwolf (Amsterdam: Elsevier), 211–233.

Leuenberger, M. C., and Filot, M. S. (2007). Temperature dependencies of high-temperature reduction on conversion products and their isotopic signatures. *Rapid Commun. Mass Spectrom.* 21, 1587–1598. doi: 10.1002/rcm.2998

Lévesque, M., Siegwolf, R., Saurer, M., Eilmann, B., and Rigling, A. (2014). Increased water-use efficiency does not lead to enhanced tree growth under xeric and Mesic conditions. *New Phytol.* 203, 94–109. doi: 10.1111/nph.12772

Li, D., Fang, K., Li, Y., Chen, D., Liu, X., Dong, Z., et al. (2017). Climate, intrinsic water-use efficiency and tree growth over the past 150 years in humid subtropical China. *PLoS One* 12:e0172045. doi: 10.1371/journal.pone.0172045

Linares, J. C., and Camarero, J. J. (2012). From pattern to process: linking intrinsic water-use efficiency to drought-induced forest decline. *Glob. Change Biol.* 18, 1000–1015. doi: 10.1111/j.1365-2486.2011.02566.x

Lindner, M., Maroschek, M., Netherer, S., Kremer, A., Barbati, A., García- Gonzalo, J., et al. (2010). Climate change impacts, adaptive capacity, and vulnerability of European forest ecosystems. *For. Ecol. Manag.* 259, 698–709. doi: 10.1016/j.foreco.2009.09.023

Loader, N. J., Robertson, I., Barker, C., Switsur, V. R., and Waterhouse, J. S. (1997). An improved technique for the batch processing of small wholewood samples to α-cellulose. *Chem. Geol.* 136, 313–317. doi: 10.1016/s0009-2541(96)00133-7

Loader, N. J., Young, G. H. F., McCarroll, D., and Wilson, R. J. S. (2013). Quantifying uncertainty in isotope dendroclimatology. *The Holocene* 23, 1221–1226. doi: 10.1177/0959683613486945

Mathias, J. M., and Hudiburg, T. W. (2022). isocalcR: an R package to streamline and standardize stable isotope calculations in ecological research. *Glob. Chang. Biol.* 28, 7428–7436. doi: 10.1111/gcb.16407

Mathias, J. M., and Thomas, R. B. (2021). Global tree intrinsic water use efficiency is enhanced by increased atmospheric CO_2 and modulated by climate and plant functional types. *Proc. Natl. Acad. Sci. USA* 118:e2014286118. doi: 10.1073/pnas.2014286118

McCabe, G. J., and Markstrom, S. L. (2007). A monthly water-balance model driven by a graphical user interface. *U. S. Geol. Surv. Open-File Rep.* 1008:12. doi: 10.3133/ofr20071088

McDowell, N. G., Allen, C. D., Anderson-Teixeira, K., Aukema, B. H., Bond-Lamberty, B., Chini, L., et al. (2020). Pervasive shifts in forest dynamics in a changing world. *Science* 368:eaaz9463. doi: 10.1126/science.aaz9463

Meeran, K., Grabner, M., Schott, K., Wächter, E., van Loo, M., and Watzinger, A. (2025). Tree size and site environment affects sessile oak growth and intrinsic water-use efficiency response to wet-dry years. *For. Ecol. Manag.* 577:122413. doi: 10.1016/j.foreco.2024.122413

Mészáros, I., Adorján, B., Nyitrai, B., Kanalas, P., Oláh, V., and Levanič, T. (2022). Long-term radial growth and climate-growth relationships of *Quercus petraea* (Matt.) Liebl. And *Quercus cerris* L. in a xeric low elevation site from Hungary. *Dendrochronologia* 76:126014. doi: 10.1016/j.dendro.2022.126014

Moore, C. E., Meacham-Hensold, K., Lemonnier, P., Slattery, R. A., Benjamin, C., Bernacchi, C. J., et al. (2021). The effect of increasing temperature on crop photosynthesis: from enzymes to ecosystems. *J. Exp. Bot.* 72, 2822–2844. doi: 10.1093/jxb/erab090

Móricz, N., Garamszegi, B., Rasztovits, E., Bidló, A., Horváth, A., Jagicza, A., et al. (2018). Recent drought-induced vitality decline of black pine (*Pinus nigra* Arn.) in south-West Hungary–is this drought-resistant species under threat by climate change? *Forests* 9:414. doi: 10.3390/f9070414

Móricz, N., Illés, G., Mészáros, I., Garamszegi, B., Berki, I., Bakacsi, Z., et al. (2021). Different drought sensitivity traits of young sessile oak (*Quercus petraea* (Matt.) Liebl.) and Turkey oak (*Quercus cerris* L.) stands along a precipitation gradient in Hungary. *For. Ecol. Manag.* 492:119165. doi: 10.1016/j.foreco.2021.119165

Móricz, N., Mészáros, I., Kern, Z., Illés, G. Z., Garamszegi, B., Eötvös, C. B., et al. (2025). Evaluating the drought tolerance of five native broadleaf tree species using dendroecological analysis in east Central Europe. *Front. For. Glob. Change* 8:1625371. doi: 10.3389/_gc.2025.1625371

Murray, F. W. (1967). On the computation of saturation vapor pressure. *J. Appl. Meteorol.* 6, 203–204. doi: 10.1175/1520-0450(1967)006<>2.0.co;2

Norton, D., Palmer, J., and Ogden, J. (1987). Dendroecological studies in New Zealand 1. An evaluation of tree age estimates based on increment cores. *N. Z. J. Bot.* 25, 373–383. doi: 10.1080/0028825X.1987.10413355

Nowacki, G. J., and Abrams, M. D. (1997). Radial-growth averaging criteria for reconstruction disturbance histories from presettlement-origin oaks. *Ecol. Monogr.* 67, 225–249. doi: 10.2307/2963514

Osmond, C. B., Bj¨orkman, O., and Anderson, D. J. (1980). "Photosynthesis," in *Physiological Processes in Plant Ecology. Toward a Synthesis with Atriplex*, eds. C. B. Osmond, O. Bj¨orkman and D. J. Anderson (Berlin, Heidelberg: Springer), 291–377.

Pasta, S., de Rigo, D., and Caudullo, G. (2016). "Quercus pubescens in Europe: distribution, habitat, usage and threats," in *European Atlas of Forest Tree Species*, eds. J. San-Miguel-Ayanz, D. Rigo, G. Caudullo, T. Houston Durrant and A. Mauri (Luxembourg: Publications Office of the European Union).

Péczely, G. (1979). *Meteorology*. Budapest: Tankönyvkiadó.

Peñuelas, J., Canadell, J. G., and Ogaya, R. (2011). Increased water-use efficiency during the 20th century did not translate into enhanced tree growth. *Glob. Ecol. Biogeogr.* 20, 597–608. doi: 10.1111/j.1466-8238.2010.00608.x

Peñuelas, J., Hunt, J. M., Ogaya, R., and Jump, A. S. (2008). Twentieth century changes of tree-ring δ13C at the southern range-edge of *Fagus sylvatica*: increasing water-use efficiency does not avoid the growth decline induced by warming at low altitudes. *Glob. Change Biol.* 14, 1076–1088. doi: 10.1111/j.1365-2486.2008.01563.x

Pernicová, N., Urban, O., Čáslavský, J., Kolář, T., Rybníček, M., Sochová, I., et al. (2024). Impacts of elevated CO2 levels and temperature on photosynthesis and stomatal closure along an altitudinal gradient are counteracted by the rising atmospheric vapor pressure deficit. *Sci. Total Environ.* 921:171173. doi: 10.1016/j.scitotenv.2024.171173

Peters, W., an der Velde, I. R., van Schaik, E., Miller, J. B., Ciais, P., Duarte, H. F., et al. (2018). Increased water-use efficiency and reduced CO_2 uptake by plants during droughts at a continental-scale. *Nat. Geosci.* 11, 744–748. doi: 10.1038/s41561-018-0212-7

R Core Team (2026). *R: A Language and Environment for Statistical Computing*. Vienna: R Foundation for Statistical Computing.

Sarris, D., Siegwolf, R., and Körner, C. (2013). Inter- and intra-annual stable carbon and oxygen isotope signals in response to drought in Mediterranean pines. *Agric. For. Meteorol.* 168, 59–68. doi: 10.1016/j.agrformet.2012.08.007

Saurer, M., Siegwolf, R. T. W., and Schweingruber, F. H. (2004). Carbon isotope discrimination indicates improving water-use efficiency of trees in northern Eurasia over the last 100 years. *Glob. Change Biol.* 10, 2109–2120. doi: 10.1111/j.1365-2486.2004.00869.x

Saurer, M., Spahni, R., Frank, D. C., Joos, F., Leuenberger, M., Loader, N. J., et al. (2014). Spatial variability and temporal trends in water-use efficiency of European forests. *Glob. Chang. Biol.* 20, 3700–3712. doi: 10.1111/gcb.12717

Saurer, M., and Voelker, S. (2022). "Intrinsic water-use efficiency derived from stable carbon isotopes of tree-rings," in *Stable Isotopes in Tree Rings: Inferring Physiological, Climatic and Environmental Responses*, eds. R. T. W. Siegwolf, J. R. Brooks, J. Roden and M. Saurer (Cham, Switzerland: Springer International Publishing), 481–498.

Scheidegger, Y., Saurer, M., Bahn, M., and Siegwolf, R. (2000). Linking stable oxygen and carbon isotopes with stomatal conductance and photosynthetic capacity: a conceptual model. *Oecologia* 125, 350–357. doi: 10.1007/s004420000466

Sen, P. K. (1968). Estimates of the regression coefficient based on Kendall's tau. *J. Am. Stat. Assoc.* 63, 1379–1389. doi: 10.1080/01621459.1968.10480934

Sternberg, L. S. L. O. R. (2009). Oxygen stable isotope ratios of tree-ring cellulose: the next phase of understanding. *New Phytol.* 181, 553–562. doi: 10.1111/j.1469-8137.2008.02661.x

Szentimrey, T. (2024). Development of new version MASHv4.01 for homogenization of standard deviation. *Időjárás* 128, 219–235. doi: 10.28974/idojaras.2024.2.5

Szentimrey, T., and Bihari, Z. (2014). *Manual of Interpolation Software MISHv1.03*. Budapest: Hungarian Meteorological Service.

Szilágyi, J., and Kovács, Á. (2010). Complementary-relationship-based evapotranspiration mapping (cremap) technique for Hungary. *Period. Polytech. Civ. Eng.* 54, 95–100. doi: 10.3311/pp.ci.2010-2.04

Timofeeva, G., Treydte, K., Bugmann, H., Rigling, A., Schaub, M., Siegwolf, R., et al. (2017). Long-term effects of drought on tree-ring growth and carbon isotope variability in Scots pine in a dry environment. *Tree Physiol.* 37, 1028–1041. doi: 10.1093/treephys/tpx041

Tognetti, R., Lombardi, F., Lasserre, B., Cherubini, P., and Marchetti, M. (2014). Tree-ring stable isotopes reveal twentieth-century increases in water-use efficiency of *Fagus sylvatica* and *Nothofagus* spp. in Italian and Chilean mountains. *PLoS One* 9:e113136. doi: 10.1371/journal.pone.0113136

van der Woude, A. M., Peters, W., Joetzjer, E., Lafont, S., Koren, G., Ciais, P., et al. (2023). Temperature extremes of 2022 reduced carbon uptake by forests in Europe. *Nat. Commun.* 14:6218. doi: 10.1038/s41467-023-41851-0

Vitasse, Y., Bottero, A., Cailleret, M., Bigler, C., Fonti, P., Gessler, A., et al. (2019). Contrasting resistance and resilience to extreme drought and late spring frost in five major European tree species. *Glob. Change Biol.* 25, 3781–3792. doi: 10.1111/gcb.14803

Wang, Z., and Wang, C. (2021). Responses of tree leaf gas exchange to elevated CO2 combined with changes in temperature and water availability: a global synthesis. *Glob. Ecol. Biogeogr.* 30, 2500–2512. doi: 10.1111/geb.13394

Wood, S. N. (2011). Fast stable restricted maximum likelihood and marginal likelihood estimation of semiparametric generalized linear models. *J. R. Stat. Soc. B* 73, 3–36. doi: 10.1111/j.1467-9868.2010.00749.x

Wood, S. N. (2017). *Generalized Additive Models: An Introduction with R*. 2nd Edn. Boca Raton, FL: Chapman and Hall/CRC.

Yee, T. W., and Mitchell, N. D. (1991). Generalized additive models in plant ecology. *J. Veg. Sci.* 2, 587–602. doi: 10.2307/3236170

Yue, S., Pilon, P., Phinney, B., and Cavadias, G. (2002). The influence of autocorrelation on the ability to detect trend in hydrological series. *Hydrol. Process.* 16, 1807–1829. doi: 10.1002/hyp.1095

Zang, C., and Biondi, F. (2015). Treeclim: an R package for the numerical calibration of proxy-climate relationships. *Ecography* 38, 431–436. doi: 10.1111/ecog.01335

Zecchin, B., Caudullo, G., and de Rigo, D. (2016). "*Acer campestre* in Europe: distribution, habitat, usage and threats," in *European Atlas of Forest Tree Species*, eds. J. San-Miguel-Ayanz, D. Rigo, G. Caudullo, T. Houston Durrant and A. Mauri (Luxembourg: Publications Office of the European Union).

Zhang, G., Bréda, N., Steil, N., Gaertner, P.-A., Levillain, J., Ruelle, J., et al. (2025). Analysing resilience of European beech tree to recurrent extreme drought events through ring growth, wood anatomy and stable isotopes. *J. Ecol.* 113, 955–973. doi: 10.1111/1365-2745.70014